Reduced cortical activity due to a shift in the balance between excitation and inhibition in a mouse model of Rett Syndrome

Vardhan S. Dani*†, Qiang Chang†‡, Arianna Maffei*, Gina G. Turrigiano*, Rudolf Jaenisch‡§¶, and Sacha B. Nelson*¶

*Department of Biology and Volen Center for Complex Systems, Brandeis University, MS 008, 415 South Street, Waltham, MA 02454-9110; ‡Whitehead Institute for Biomedical Research, 9 Cambridge Center, Cambridge, MA 02142; and §Department of Biology, Massachusetts Institute of Technology, 77 Massachusetts Avenue, Cambridge, MA 02139-4307

Contributed by Rudolf Jaenisch, July 18, 2005

Rett Syndrome (RTT) is a devastating neurological disorder that is caused by mutations in the *MECP2* gene. *Mecp2*-mutant mice have been used as a model system to study the disease mechanism. Our previous work has suggested that MeCP2 malfunction in neurons is the primary cause of RTT in the mouse. However, the neurophysiological consequences of MeCP2 malfunction remain obscure. Using whole-cell patch-clamp recordings in cortical slices, we show that spontaneous activity of pyramidal neurons is reduced in *Mecp2*-mutant mice. This decrease is not caused by a change in the intrinsic properties of the recorded neurons. Instead, the balance between cortical excitation and inhibition is shifted to favor inhibition over excitation. Moreover, analysis of the miniature excitatory postsynaptic currents (mEPSCs)/inhibitory postsynaptic currents (mIPSCs) in the *Mecp2*-mutant cortex reveals a reduction in mEPSC amplitudes, without significant change in the average mIPSC amplitude or frequency. These findings provide the first detailed electrophysiological analysis of *Mecp2*-mutant mice and provide a framework for understanding the pathophysiology of the disease and tools for studying the underlying disease mechanisms.

autism | cortical circuit | MeCP2 | mental retardation

Rett Syndrome (RTT) is a pervasive neurodevelopmental disorder associated with mental retardation, autistic behavior, and loss of previously acquired skills, including purposeful hand use and expressive language (1). Affected individuals begin to acquire motor and cognitive function normally but then regress after 6–18 months. The disease is sex-linked and is due, in most cases, to abnormal function of a single gene, the methyl CpG-binding protein *MECP2* (2). Deletion of all, or the third exon, of the *Mecp2* gene produces functional nulls and recapitulates, in mice, many features of the human disorder (3, 4). Mice with truncated MeCP2 also recapitulate many RTT features (5). *Mecp2*-null mice are normal until 5 weeks of age, when they begin to exhibit abnormal behavior resembling symptoms observed in RTT patients. Brain-specific *Mecp2*-mutant mice show pathological symptoms identical to those found in the germline *Mecp2*-null mice, thereby implicating MeCP2 malfunction in the brain as the primary cause of RTT (3). Transgenic expression of MeCP2 in postmitotic neurons in the *Mecp2*-mutant mice rescues the RTT phenotype (6). Overexpression of MeCP2 in postmitotic neurons in WT mice also causes behavioral and physiological abnormalities (6, 7). Taken together, these data strongly argue for the importance of MeCP2 function during the normal maturation and refinement of neural circuits, which may be compromised in *Mecp2*-mutant mice.

Despite profound behavioral abnormalities and premature death, the neuropathological phenotype is remarkably subtle in *Mecp2*-mutant mice. The mutant brain weighs ≈20–25% less than the WT. Mutant hippocampal CA2 pyramidal neurons are ≈15–25% smaller than WT neurons (3). Mutant neocortical projection neurons have simplified dendritic arbors (8). Yet, other gross morphological features of the CNS are preserved. In addition, although MeCP2 is hypothesized to function as a global repressor of transcription, expression-profiling studies have revealed only subtle changes in gene expression (9). These studies suggest that a more functional approach is needed to understand the nature of the cortical dysfunction caused by MeCP2 malfunction. Consequently, we undertook an electrophysiological analysis of cortical circuit function in *Mecp2*-null mice. By using whole-cell patch-clamp recordings from layer 5 (L5) pyramidal neurons in slices of the primary somatosensory cortex (S1), we observed reduced spontaneous firing at both early symptomatic stages, and presymptomatic stages, as early as the second postnatal week. The decrease in firing rate was not accompanied by a change in the intrinsic excitability of these cells. Instead, the total excitatory synaptic drive onto L5 pyramidal cells was decreased, whereas the total inhibitory drive was increased. Analysis of action-potential-independent postsynaptic currents revealed smaller miniature excitatory postsynaptic currents (mEPSCs) in *Mecp2* mutant neurons compared with WT controls. Thus, our results show that the balance between excitation and inhibition in a major class of cortical neurons is shifted to favor inhibition over excitation in *Mecp2*-mutant mice. Similar changes in other regions of the brain could underlie some of the cognitive, motor, social, and linguistic symptoms observed in RTT patients.

Methods

Animals. WT male mice were bred with female mice heterozygous for a *Mecp2*-mutant allele (3) to generate male mutant mice and WT littermate controls. Experimental mice were genotyped by using a PCR assay, as described in ref. 3. All animals were in a mixed background (129, C57BL/6 and BALB/c). All procedures for animal handling were approved by the Animal Care and Use Committee of Brandeis University.

Solutions. The standard artificial cerebrospinal fluid (ACSF) contained 126 mM NaCl, 3 mM KCl, 2 mM $MgSO_4$, 1 mM $NaHPO_4$, 25 mM $NaHCO_3$, 2 mM $CaCl_2$, and 14 mM dextrose. For spontaneous firing and synaptic current recordings, the ACSF was modified as follows: 3.5 mM KCl and 0.5 mM $MgCl_2$ (in place of $MgSO_4$) and 1 mM $CaCl_2$. Osmolality was adjusted to 318 ± 2 mOsm.

Slices. Coronal sections (300 μm thick) containing the S1 were cut in cold ACSF by using a Leica VT1000S slicer. Slices were

Abbreviations: ACSF, artificial cerebrospinal fluid; APV, 2-amino-5-phosphonovaleric acid; DNQX, 6,7-dinitroquinoxaline-2,3-dione; L5, layer 5; mEPSC, miniature excitatory postsynaptic current; mIPSC, miniature inhibitory postsynaptic current; P, postnatal day; RTT, Rett Syndrome; S1, primary somatosensory cortex; TTX, tetrodotoxin.

†V.S.D. and Q.C. contributed equally to this work.

¶To whom correspondence may be addressed. E-mail: nelson@brandeis.edu or jaenisch@wi.mit.edu.

www.pnas.org/cgi/doi/10.1073/pnas.0506071102

incubated in standard ACSF at 37°C for 15–20 min immediately after slicing and, subsequently, at room temperature. For spontaneous firing (current-clamp) and current recordings (voltage-clamp), slices were preincubated (≈45 min) and perfused in modified ACSF, as described in ref. 10.

Drugs. For intrinsic excitability studies, the standard ACSF contained a mixture of the following synaptic blockers: 50 μM 2-amino-5-phosphonovaleric acid (APV), 20 μM 6,7-dinitroquinoxaline-2,3-dione (DNQX), and 20 μM bicuculine. For mEPSC recordings, the standard ACSF contained 0.1 μM tetrodotoxin (TTX), 20 μM bicuculine, and 50 μM APV. For miniature inhibitory postsynaptic current (mIPSC) recordings, the standard ACSF contained 0.1 μM TTX, 20 μM DNQX, and 50 μM APV.

Pipette Internal Solutions. Whole-cell pipette solution for current-clamp and mEPSC voltage-clamp recordings contained 20 mM KCl, 100 mM potassium gluconate, 10 mM Hepes, 0.1% biocytin, 4 mM MgATP, 0.3 mM NaGTP, and 10 mM sodium phosphocreatinine. For measuring spontaneous synaptic currents, the internal solution contained 20 mM KCl, 100 mM cesium methyl sulfonate, 10 mM Hepes, 0.1% biocytin, 4 mM MgATP 4, 0.3 mM NaGTP, 10 mM sodium phosphocreatinine, and 3 mM QX-314. For measuring mIPSCs, KCl in the pipette solution was substituted for potassium gluconate, so that the calculated chloride-reversal potential was 0 mV.

Electrophysiology. Somatic whole-cell recordings were obtained from visually identified L5 pyramidal cells, as described in ref. 11. Glass pipette electrodes (4- to 6-MΩ resistance) were pulled from borosilicate capillaries (World Precision Instruments, Sarasota, FL) by using a Sutter P92 Flame/Brown Puller (Sutter Instruments, Novato, CA). All data acquisition and analysis was performed by using the program IGOR PRO (WaveMetrics, Lake Oswego, OR) and in-house programs. Cells were not used for analysis if resting membrane potential (V_m) was more depolarized than −60 mV, access resistance >25 MΩ (20 MΩ for mEPSC recordings), or input resistance (R_{in}) <50 MΩ or if any of these parameters changed by >20% during data acquisition. Data were acquired by using a Multiclamp 700A computer-controlled amplifier (Axon Instruments, Union City, CA/Molecular Devices) at 10 kHz and low-pass filtered at 3 kHz. For spontaneous firing recordings in modified ACSF, a small depolarizing current was applied to adjust the interspike potential to −60 mV. Intrinsic excitability of L5 pyramidal neurons was assessed by measuring the firing rate in response to a series of depolarizing pulses, in the presence of synaptic blockers. The spike-voltage threshold was computed as the point before the peak of the first derivative of the membrane potential at which the third derivative flipped from negative to positive (12). Spontaneous excitatory and inhibitory synaptic currents were recorded in the same cells in modified ACSF by voltage-clamping the membrane potential at the reversal potential of one of the two postsynaptic currents (−60 to −50 mV for GABAergic currents and 5–15 mV for glutamergic currents), measured independently in each cell by clamping the membrane at different potentials in 5-mV increments. mEPSCs and mIPSCs were measured at −70 mV. In all experiments, slices were fixed and stained for biocytin to confirm the identity of the recorded cells.

All data reported in the text and bar plots in Figs. 1–5 represent the mean (±SEM).

Results

Reduced Circuit Activity in L5 Pyramidal Neurons of *Mecp2*-Null Mice. *Mecp2*-mutant mice exhibit many abnormal behaviors that mimic those observed in human RTT patients. Yet, the neural basis of these abnormalities remains unclear. To identify the neuronal functions compromised in these mutant mice, we examined activity and basic properties of synaptic transmission within local cortical microcircuits. To maximize our chances of finding a defect, we first studied *Mecp2*-mutant mice at an early symptomatic phase [postnatal day (P) 30–P 35]. To determine whether or not the overall excitability of local cortical circuits is altered after the loss of MeCP2 function, we measured spontaneous action-potential firing in neocortical slices obtained from *Mecp2*-mutant and WT littermate control male mice. Whole-cell current-clamp recordings were obtained from thick-tufted L5 pyramidal cells in the S1 at room temperature (25 ± 1°C). We recorded from L5 pyramidal neurons, because these are among the neurons that exhibit subtle alterations in morphology in RTT patients and *Mecp2*-mutant mice (3, 13, 14). Slices incubated in standard ACSF typically exhibit very low levels of spontaneous activity. However, when placed in modified ACSF (see *Methods*) containing reduced Mg^{2+} (one-fourth, compared with standard ACSF) and Ca^{2+} (one-half) and slightly elevated potassium (15), L5 pyramidal neurons fired spontaneously at 0.01–8 Hz. The changes in ACSF ionic composition may enhance NMDA-receptor-dependent synaptic transmission, reduce calcium-dependent potassium currents, and reduce short-term synaptic depression, relative to that observed with standard ACSF. The modified ACSF is, in some respects, more similar to *in vivo* rodent CSF than to standard ACSF (16, 17). We have shown previously that experience-dependent changes in circuit excitability can be readily revealed under these "active-slice" conditions (10). Our recordings included both bursting and regular spiking pyramidal neurons. Analysis of spontaneous firing of L5 pyramids revealed an ≈4-fold reduction in the mean firing rate of *Mecp2*-mutant neurons, compared with WT [Fig. 1 *A* and *B*; WT 3.15 ± 0.47 Hz, $n = 20$; mutant, 0.75 ± 0.25 Hz, $n = 22$, $P < 0.001$ (two-tailed Student's t test)]. This decreased firing rate of mutant neurons was also observed when recordings were performed with the same age group of mice but at temperatures closer to physiological conditions i.e., 31–33°C [Fig. 1*C*, $P < 0.001$ (WT, $n = 15$; mutant, $n = 7$)].

Reduced Cortical Activity Precedes Behavioral Symptoms. *Mecp2*-mutant mice develop symptoms of hind-limb clasping, abnormal gait, and reduced locomotor activity, beginning at ≈4–5 weeks of age. Neuropathological changes in dendritic complexity are not present at 2 weeks but become evident by 8 weeks (8). To determine whether changes in cortical excitability precede or follow other symptoms, we performed recordings of spontaneous activity in WT and mutant mice at earlier ages.

Recordings performed at 2 or 3 weeks of age also revealed reduced spontaneous firing of neurons from mutant animals, although the reduction was only ≈2-fold, compared with WT (Fig. 1*D*, P 14–P 16; WT, 2.23 ± 0.44 Hz, $n = 19$; mutant, 1.09 ± 0.35 Hz, $n = 19$; Fig. 1*E*, P 21–P 24; WT, 2.42 ± 0.36 Hz, $n = 20$; mutant, 1.37 ± 0.29 Hz, $n = 24$; $P < 0.04$). Thus, the observed decrease in the firing rate of L5 neurons is a milder, yet detectable, phenotype in the *Mecp2*-mutant mice well (up to 2 weeks) before the onset of anatomical and behavioral symptoms.

Normal Intrinsic Excitability in Mutant Neurons. Reduced circuit excitability could arise from three different types of physiological changes that are not mutually exclusive. These include (*i*) reduced intrinsic electrical excitability of L5 pyramidal neurons, (*ii*) decreased excitatory synaptic drive onto these pyramidal neurons, or (*iii*) increased inhibitory synaptic drive onto these pyramidal neurons. To determine whether intrinsic or synaptic conductances were altered in the mutants, we measured the electrical responses of L5 pyramidal neurons to current injection in the presence of pharmacological blockers of excitatory and inhibitory synaptic transmission (APV, DNQX, and bicuculine). A series of 500-ms depolarizing current steps were injected to

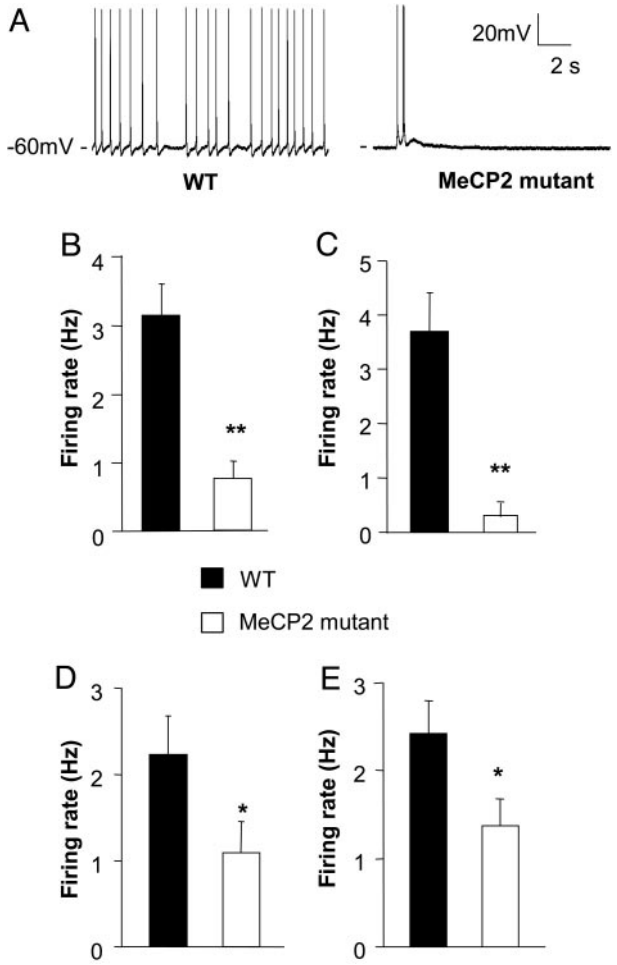

Fig. 1. Spontaneous firing of L5 pyramidal neurons in S1 is reduced in *Mecp2* mutants, compared with WT controls. (*A*) Representative spontaneous firing recordings at room temperature (25 ± 1°C) from a WT (*Left*) and *Mecp2*-mutant cell (*Right*). (*B*) Average spontaneous firing rate of WT and mutants. The ≈4-fold difference in mean firing rate of WT and mutant was statistically significant (Student's *t* test, $P < 0.001$). (*C*) Recordings performed at closer to physiological temperature (31–33°C) also showed a decreased firing rate in mutants. (*D* and *E*) Smaller reductions in spontaneous firing rate at presymptomatic ages. Mean firing rate was reduced ≈2-fold in presymptomatic mice at P 14–P 16 (*D*), or at P 21–P 24 (*E*). Statistical significance is indicated by * for $P < 0.05$ and ** for $P < 0.01$.

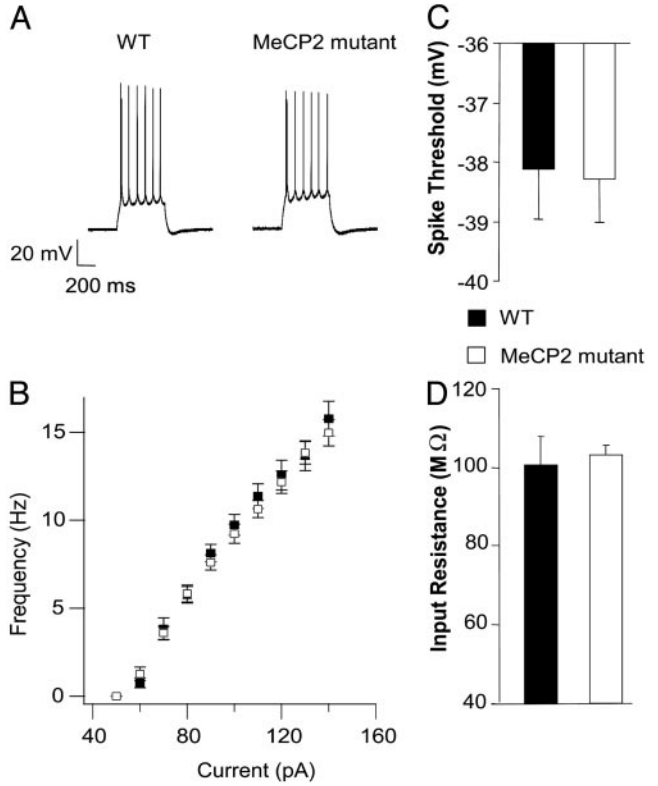

Fig. 2. Intrinsic excitability of L5 neurons from *Mecp2* mutants is unchanged. All recordings are from 4- to 5-week-old mice. Slices were continuously perfused in standard ACSF (at room temperature) containing APV, DNQX, and bicuculine. (*A*) Sample traces of spikes evoked by a depolarizing current step of 130 pA in a WT (*Left*) and a mutant (*Right*) L5 cell. (*B*) Mean firing rate vs. injected current amplitude (F–I curve). The mutant and WT F–I curves are almost identical. The mean first spike threshold (*C*) and input resistance (*D*) of mutant cells ($n = 12$) were not significantly different from WT cells ($n = 12$).

elicit action potentials (Fig. 2*A*), and the resulting firing rates were plotted as a function of increasing current amplitude (F–I curves). Our analysis was restricted to regular spiking (nonbursting) pyramidal cells in L5. The F–I curves for WT and mutant neurons were almost identical to each other (Fig. 2*B*, WT, $n = 12$; mutant, $n = 12$). The mean voltage threshold for triggering the first spike during the depolarizing step was unchanged between the two conditions (Fig. 2*C*). The input resistance (R_{in}), measured regularly for each cell throughout the duration of the recording, was also very similar between WT and mutant cells (Fig. 2*D*). These data show that the intrinsic electrical properties of mutant neurons are not significantly altered. Previous work in our lab has shown that spontaneous firing is almost entirely blocked in modified ACSF when glutamatergic and GABAergic synapses are blocked (10). Thus, changes in intrinsic properties, if any, are unlikely to contribute to the observed difference in spontaneous firing rates.

Deletion of *Mecp2* Shifts the Balance Between Excitation and Inhibition. Reduced activity in the face of normal cellular excitability suggests that the balance between total excitatory synaptic drive and total inhibitory synaptic drive onto L5 pyramids is altered in the *Mecp2* mutants. To further test this possibility, we measured spontaneous excitatory and inhibitory synaptic currents in the presence of ongoing network activity within the slices (i.e., without blockade of action potentials and synaptic receptors). To separate excitatory and inhibitory currents within the same cell, we recorded excitatory currents (Fig. 3*A*) by voltage-clamping the cell membrane at the measured chloride-reversal potential (E_{Cl}) (WT, $E_{Cl} = -56.7 \pm 1.1$ mV; *Mecp2*-mutant, $E_{Cl} = -57.1 \pm 0.7$ mV, $P = 0.76$, *t* test), and inhibitory currents (Fig. 3*C*) at the measured excitatory postsynaptic current reversal potential (WT, 10.3 ± 0.7 mV; *Mecp2* mutant, 9.2 ± 0.8 mV; $P = 0.27$, *t* test). At E_{Cl}, there were virtually no outward currents, suggesting that spontaneous activity in the slice does not activate appreciable $GABA_B$ currents, which reverse at more hyperpolarized potentials. The total excitatory and inhibitory synaptic charge was calculated by integrating the respective baseline subtracted postsynaptic currents over 150 s. Individual events were not measured because of the high degree of overlap between spontaneous events. The mean excitatory synaptic charge was decreased (Fig. 3*B*, WT, $n = 12$; mutant, $n = 12$; $P < 0.01$), and the mean inhibitory synaptic charge was increased significantly in mutant neurons (Fig. 3*D*, WT, $n = 12$; mutant, $n = 12$; $P < 0.05$). These data show that there is a marked change in the spontaneous excitatory and inhibitory synaptic input onto L5 pyramidal cells in *Mecp2*-mutant mice. This shift in the balance between excitation and inhibition reduces net excitatory

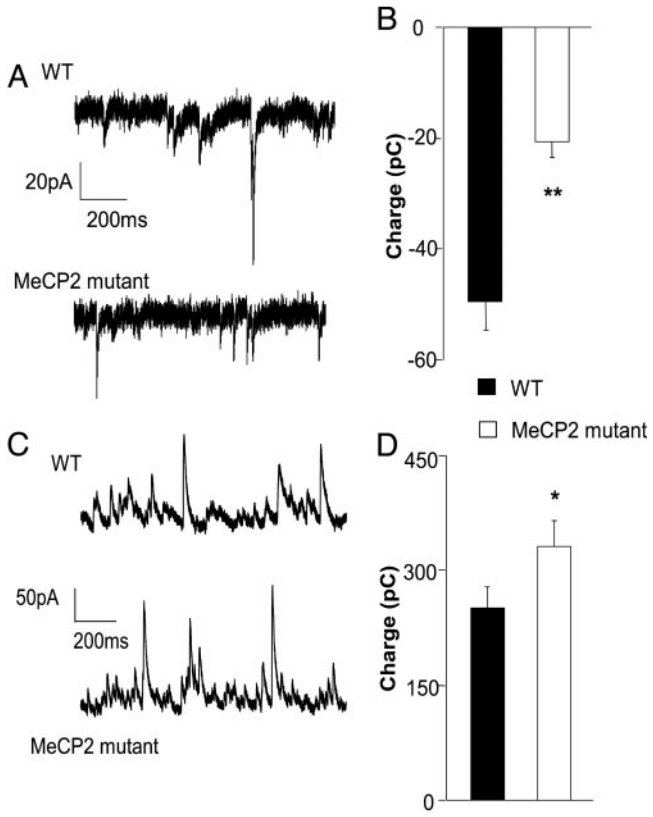

Fig. 3. The balance between excitation and inhibition onto L5 pyramidal neurons is altered in *Mecp2* mutants. Recordings were made in the presence of ongoing spontaneous activity. Total excitatory and inhibitory synaptic charge was calculated by integrating baseline subtracted spontaneous synaptic current. (*A*) Representative recordings of spontaneous excitatory postsynaptic currents (EPSCs) (recorded at the chloride-reversal potential) from L5 pyramidal neurons in slices from 4- to 5-week-old WT and mutant mice in modified ACSF. (*B*) The average excitatory charge is reduced in mutant mice ($n = 12$ for WT and mutants; $P < 0.01$, Student's t test) Representative recordings of spontaneous inhibitory postsynaptic currents (IPSCs) (recorded at the reversal potential for spontaneous EPSCs. (*C*) Representative recordings of spontaneous IPSCs (recorded at the reversal potential for spontaneous EPSCs. (*D*) The average inhibitory charge recorded from the same cells as in *C* is increased, compared with WT controls ($n = 12$ for WT and mutant, $P < 0.05$, t test).

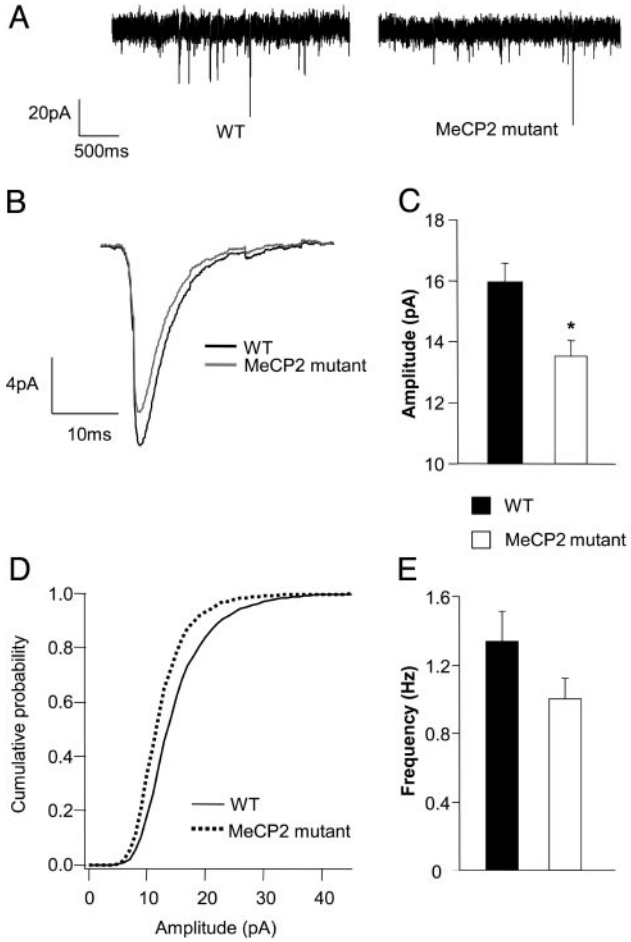

Fig. 4. Reduced amplitude of excitatory quantal transmission in L5 pyramids of 4- to 5-week-old *Mecp2*-mutant mice. mEPSCs recorded from L5 pyramidal cells in the presence of APV, bicuculine, and TTX. (*A*) Sample traces from WT and mutant cells voltage clamped at −70 mV. (*B*) Averaged mEPSC from 12 WT and 12 mutant cells. (*C*) mEPSC amplitude was reduced by 15%, and this difference was statistically significant ($P < 0.01$, t test). (*D*) Cumulative histograms of 300 events from each of 12 WT cells and 12 mutant cells showed a significant leftward shift in the mEPSC amplitude for mutant cells. (*E*) a small reduction in the mean mEPSC frequency was observed in mutants was not statistically significant ($P = 0.12$, t test).

drive and may, therefore, contribute to the observed decrease in spontaneous firing rates in these cells.

Quantal Excitatory Transmission Is Modestly Reduced. Reduced excitatory transmission could reflect a reduction in the quantal response to the release of individual glutamatergic vesicles, a reduced average rate of vesicle release, or both. To assess possible changes in quantal responses, we studied action-potential-independent spontaneous mEPSCs. AMPA-receptor-mediated mEPSCs were recorded in the presence of TTX, APV, and bicuculine during voltage-clamp at −70 mV. Analysis of peak amplitudes of 300 randomly selected mEPSCs from each cell revealed a small but significant decrease in the mean mEPSC peak amplitude of *Mecp2*-mutant cells (Fig. 4 *B* and *C*). A marked shift in the histogram distribution toward lower amplitudes was observed for mutant cells. Construction of a cumulative probability histogram, using the same 300 selected events per cell, revealed that this decrease in mEPSC amplitude in mutant cells was significant, compared with WT (Fig. 4*D*; $P = 4 \times 10^{-62}$, Kolgomorov–Smirnov test). The average area (charge) was also significantly lower in *Mecp2*-mutant cells (Table 1). Although the cumulative histograms of interevent intervals (IEI) were significantly different between WT and mutant mEPSCs (Kolgomorov–Smirnov test, $P = 1.7 \times 10^{-17}$, data not shown), the mean IEI and corresponding event frequencies computed for individual neurons were not statistically significantly different between the two conditions (Fig. 4*E*). The small difference in frequency was still present when mutant mEPSC recordings were scaled up to have the same average amplitude as WT, and events were redetected. Hence, the apparent difference is not due simply to poorer detection caused by a decrease in mEPSC amplitude. The decreases in mEPSC peak amplitude and charge in mutant cells are smaller than, but may contribute to, the reduced spontaneous excitatory synaptic charge observed in active slices.

To determine whether or not increased spontaneous inhibitory synaptic currents were caused in part by enhanced quantal responses to release of GABA vesicles, mIPSCs were recorded by clamping the cell membrane at −70 mV and using pipette internal solution that changes the Cl^- reversal potential of the cell to ≈0 mV. Fig. 5*A* shows sample recordings of mIPSCs from a WT and a mutant cell. The average mIPSC peak amplitude was

NEUROSCIENCE

Table 1. Average parameters for mEPSC and mIPSC recordings

	mEPSCs		mIPSCs	
Parameters	WT	Mutant	WT	Mutant
Frequency, Hz	1.3 ± 0.17	1.0 ± 0.12	5.97 ± 0.8	7.03 ± 0.5
Peak amplitude, pA	15.9 ± 0.6	13.5 ± 0.5*	35.1 ± 3.0	40.6 ± 3.1
Rise time, ms	1.22 ± 0.03	1.15 ± 0.025*	0.81 ± 0.04	0.67 ± 0.04*
τ_{Decay}, ms	4.28 ± 0.12	4.18 ± 0.1	7.5 ± 0.32	6.6 ± 0.23*
Average area, fC	−70.4 ± 4.1	−53.4 ± 2.6*	−316.1 ± 26.2	−337.8 ± 24.1
V_m, mV	−65.9 ± 0.7	−67.1 ± 0.9	−66.4 ± 0.5	−66.9 ± 0.6
R_m, MΩ	87.4 ± 5.5	101.0 ± 3.6	110.1 ± 13.2	117 ± 8.7
C_m, pF	168.6 ± 10.7	148.7 ± 4.7	98.2 ± 6.1	90.2 ± 6.4
R_s, MΩ	15.1 ± 0.66	16.2 ± 0.6	19.9 ± 0.9	20.6 ± 0.8

*Indicates statistical significance between WT and mutant by Student's *t* test with $P < 0.05$ or less. V_m, resting membrane potential; R_{in}, input resistance; τ_{Decay}, decay time; C_m, membrane capacitance; R_s, series resistance.

higher in mutant cells, but the difference between the means was not statistically significant (Fig. 5 *B* and *C*, $P = 0.23$, *t* test). Cumulative histograms of peak amplitudes of the first 300 selected events from each cell showed a shift to larger amplitudes for mutant cells that was statistically significant (Fig. 5*D*, $P = 1.9 \times 10^{-9}$, Kolgomorov–Smirnov test). The mean frequency of mIPSCs was not significantly different between the two conditions (Fig. 5*E*). However, the mean frequency of high amplitude events (>30 pA) was significantly increased in *MeCP2* mutants (WT, 1.96 ± 0.42 Hz; *MeCP2*-mutant mice, 2.91 ± 0.33 Hz; $P < 0.05$, *t* test, data not shown). The average decay time constant (τ_{decay}) showed a small but significant decrease in the mutant mice (Table 1).

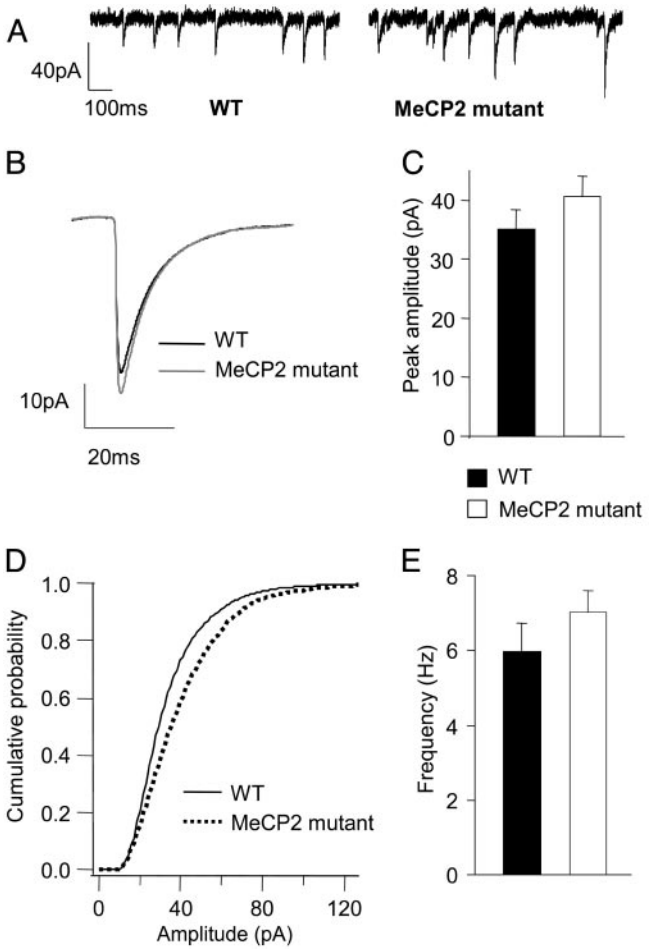

Fig. 5. Subtle differences in unitary IPSCs in L5 pyramids of 4- to 5-week-old *Mecp2* mutant mice. mIPSCs recorded from L5 pyramidal cells in the presence of APV, DNQX, and TTX. (*A*) Sample traces from WT and mutant cells voltage-clamped at −70 mV. (*B*) Averaged mIPSC from 17 WT and 17 mutant cells. The slightly increased mIPSC amplitude in mutant cells was not statistically significant across cells (*C*) ($P = 0.23$, *t* test), although the cumulative histograms of events from WT and mutant cells (*D*) showed a skew toward larger amplitudes that was highly significant. There was no significant change in the mean mIPSC frequency (*E*) and a small but significant change in the mean decay time constant (Table 1).

Discussion

Reduced Cortical Activity Precedes the Onset of Overt Symptoms and Is Progressive. Similar to human RTT patients, *Mecp2*-mutant mice are born normal and enjoy a window of apparently normal postnatal development before the onset of the disease. However, MeCP2 expression in WT mice starts very early in the brain during embryonic development and peaks in many regions of the brain before the onset of the disease. Although it is possible that MeCP2 function is not required during early development of the brain, many have suspected that some aspects of neuronal function are already compromised in *Mecp2*-mutant mice before the appearance of classic behavioral symptoms. We reported here that, at 2 weeks of age, L5 pyramidal neurons in slices of the S1 in *Mecp2*-mutant mice were only half as active as those in the WT cortex. This finding provides experimental evidence for a physiological abnormality preceding the onset of overt symptoms in *Mecp2*-mutant mice.

The reduced cortical activity is progressive, because the difference between mutant and WT animals was only ≈2-fold at 2–3 weeks but was ≈4-fold at 4–5 weeks, when animals begin to exhibit symptoms. During normal development through this time window, firing rates of cortical pyramidal neurons are homeostatically regulated by complex changes in excitatory or inhibitory circuitry (10, 18, 19). Normally, lowered spontaneous activity, such as that occurring during sensory deprivation, results in increased recurrent excitation and reduced inhibition. The fact that this does not occur in the mutant animals suggests that either changes induced by loss of *Mecp2* overwhelm the normal homeostatic mechanisms, or the homeostatic mechanisms themselves have been disrupted.

Mechanisms of Reduced Cortical Activity. The reduced circuit activity assayed by measuring the spontaneous firing of L5 pyramidal neurons was not accompanied by any changes we could detect in the intrinsic electrophysiological properties of those neurons. CNS neurons must carefully balance expression of their inward and outward ionic conductances to achieve their characteristic threshold, firing rates as a function of current (F–I) curve, and input resistance. The fact that these parameters did

not change suggests that a large part of the cell's physiology remains unaltered by deletion of *Mecp2*.

Reduced circuit excitability was accompanied by both reduced spontaneous excitatory synaptic input and increased inhibition. The recurrent nature of cortical circuitry greatly complicates the problem of identifying the circuit elements responsible for a change in overall circuit excitability. For example, enhanced inhibition could also reduce spontaneous excitatory postsynaptic currents by preventing presynaptic excitatory neurons from firing. This is apparently not the whole story, however, because, in the absence of action potentials and inhibition, mEPSCs are reduced. The fact that the reduction of spontaneous excitatory postsynaptic currents is larger (58%) than the reduction of mEPSCs (15%) could reflect the added effects of inhibition or could simply reflect the amplifying effect of recurrent excitation. In other words, a small reduction in mini amplitude could lead to less firing, which then produces a larger decrease in spontaneous excitation. In addition, it is possible that there are also effects of MeCP2 on the number or strength of unitary excitatory connections (10).

The observed increase in spontaneous inhibitory postsynaptic currents was not accompanied by a significant increase in average quantal inhibitory transmission. There was a significant shift of the mutant mIPSC amplitude distribution to the right, but this affected primarily the larger events. The small (16%) increase in mIPSC amplitude could have contributed to the larger (32%) increase in spontaneous inhibitory postsynaptic charge but was not by itself significant. Other factors, such as increased excitatory input to interneurons or changes in the number or strength of inhibitory connections are also likely to have played a role. Taken together, our data suggest that loss of MeCP2 affects multiple aspects of cortical circuitry that, together, produce a state of reduced excitability and decreased activity.

Implications for RTT Disease Mechanisms. The signaling pathways that link the lack of MeCP2 to a shift in the balance between excitation and inhibition remain obscure. It is not hard to imagine, however, how such a shift favoring inhibition and reduced activity in cortical circuits could produce some of the symptoms associated with loss of MeCP2 function in mice and humans. *Mecp2*-null mice exhibit reduced locomotor activity. Reduced excitatory drive of L5 projection neurons, particularly if it extends beyond S1 to include primary and supplementary motor areas, may reduce the relay of cortical activity to the spinal cord and other motor centers. If the physiological changes observed in the mouse model are also present in human RTT patients, reduced cortical activity in cortical regions subserving skilled motor behaviors and language could contribute to the impairment of these behaviors in the disease.

A shift in the balance between excitation and inhibition may also underlie deficits in learning and memory in mutant mice and human RTT patients. Long-term potentiation (LTP) and other forms of cortical synaptic plasticity at excitatory synapses are profoundly suppressed by concurrent activation of inhibition (11, 20). In a mouse model of another neurodevelopmental retardation disorder Down Syndrome, hippocampal LTP is reduced due to enhanced inhibition (21). Reduced hippocampal LTP has also been observed in *Mecp2*-mutant mice (7). Similar effects could potentially contribute to impaired learning and cognitive abilities in RTT patients.

We thank Jessie Dausman and Ruth Flannery for assistance with mouse work, Robert Cudmore and Ken Sugino for providing analysis programs, and Roman Pavlyuk for histology work. This work was supported by a McKnight Foundation grant. Q.C. was supported by a postdoctoral fellowship from the Rett Syndrome Research Foundation, and R.J. was supported by a Grants of Excellence for Accelerated Rett Research award from the Rett Syndrome Research Foundation.

1. Hagberg, B. (1997) *Eur. Child Adolesc. Psychiatry* **6,** Suppl. 1, 2–4.
2. Amir, R. E., Van den Veyver, I. B., Wan, M., Tran, C. Q., Francke, U. & Zoghbi, H. Y. (1999) *Nat. Genet.* **23,** 185–188.
3. Chen, R. Z., Akbarian, S., Tudor, M. & Jaenisch, R. (2001) *Nat. Genet.* **27,** 327–331.
4. Guy, J., Hendrich, B., Holmes, M., Martin, J. E. & Bird, A. (2001) *Nat. Genet.* **27,** 322–326.
5. Shahbazian, M., Young, J., Yuva-Paylor, L., Spencer, C., Antalffy, B., Noebels, J., Armstrong, D., Paylor, R. & Zoghbi, H. (2002) *Neuron* **35,** 243–254.
6. Luikenhuis, S., Giacometti, E., Beard, C. F. & Jaenisch, R. (2004) *Proc. Natl. Acad. Sci. USA* **101,** 6033–6038.
7. Collins, A. L., Levenson, J. M., Vilaythong, A. P., Richman, R., Armstrong, D. L., Noebels, J. L., Sweatt, J. D. & Zoghbi, H. Y. (2004) *Hum. Mol. Genet.* **13,** 2679–2689.
8. Kishi, N. & Macklis, J. D. (2004) *Mol. Cell. Neurosci.* **27,** 306–321.
9. Tudor, M., Akbarian, S., Chen, R. Z. & Jaenisch, R. (2002) *Proc. Natl. Acad. Sci. USA* **99,** 15536–15541.
10. Maffei, A., Nelson, S. B. & Turrigiano, G. G. (2004) *Nat. Neurosci.* **7,** 1353–1359.
11. Sjöström, P. J., Turrigiano, G. G. & Nelson, S. B. (2001) *Neuron* **32,** 1149–1164.
12. Henze, D. A., Gonzalez-Burgos, G. R., Urban, N. N., Lewis, D. A. & Barrionuevo, G. (2000) *J. Neurophysiol.* **84,** 2799–2809.
13. Armstrong, D., Dunn, J. K., Antalffy, B. & Trivedi, R. (1995) *J. Neuropathol. Exp. Neurol.* **54,** 195–201.
14. Armstrong, D. D., Dunn, K. & Antalffy, B. (1998) *J. Neuropathol. Exp. Neurol.* **57,** 1013–1017.
15. Sanchez-Vives, M. V. & McCormick, D. A. (2000) *Nat. Neurosci.* **3,** 1027–1034.
16. Chutkow, J. G. (1974) *Mayo Clin. Proc.* **49,** 244–247.
17. Zhang, E. T., Hansen, A. J., Wieloch, T. & Lauritzen, M. (1990) *J. Cereb. Blood Flow Metab.* **10,** 136–139.
18. Desai, N. S., Rutherford, L. C. & Turrigiano, G. G. (1999) *Nat. Neurosci.* **2,** 515–520.
19. Turrigiano, G. G. & Nelson, S. B. (2004) *Nat. Rev. Neurosci.* **5,** 97–107.
20. Bear, M. F., Press, W. A. & Connors, B. W. (1992) *J. Neurophysiol.* **67,** 841–851.
21. Kleschevnikov, A. M., Belichenko, P. V., Villar, A. J., Epstein, C. J., Malenka, R. C. & Mobley, W. C. (2004) *J. Neurosci.* **24,** 8153–8160.